Localized Collective Excitations in Superfluid Helium in Vycor

R. M. Dimeo,[1] P. E. Sokol,[1] C. R. Anderson,[2,3] W. G. Stirling,[2] K. H. Andersen,[3] and M. A. Adams[4]

[1]*Department of Physics, The Pennsylvania State University, University Park, Pennsylvania 16802*
[2]*Department of Physics, University of Liverpool, Liverpool, L69 7ZE, United Kingdom*
[3]*Institut Laue-Langevin, BP 156, 38042 Grenoble Cédex 9, France*
[4]*ISIS Facility, Rutherford Appleton Laboratory, Chilton, Didcot, Oxon, OX11 0QX, United Kingdom*
(Received 1 June 1998)

Inelastic neutron scattering has been used to probe the collective excitations of superfluid helium in porous Vycor glass for $0.5 \leq T(K) \leq 1.9$. The confined roton displays a temperature dependence similar to that of the bulk roton but with larger widths. Additional scattering has been observed near the roton minimum but with a substantially lower energy than the bulk roton. This scattering is consistent with a "two-dimensional roton," predicted to occur at the solid-liquid interface and inferred from measurements of the heat capacity and superfluid fraction. [S0031-9007(98)08080-6]

Superfluid helium is a model system whose microscopic excitations explain the macroscopic thermodynamic and transport properties of the liquid [1]. The superfluid excitation spectrum at low momentum transfers ($Q < 2.4$ Å^{-1}) is well defined, clearly showing the quantum nature of the liquid via the long-lived excited states. The dominant excitations, which determine the thermodynamics of the liquid, are the phonons at low Q ($Q < 0.9$ Å^{-1}) and the rotons at higher Q ($Q \simeq 1.9$ Å^{-1}). At low temperatures ($T < 0.7$ K) the liquid can be treated as a noninteracting gas of phonons, and above 1 K the liquid can be treated as an ideal gas of rotons.

Confinement can have dramatic effects on the macroscopic properties of superfluid helium, especially near the superfluid transition temperature. For instance, confinement in aerogel glass results in only a slight decrease in the transition temperature T_λ but dramatically changes the critical exponent [2]. Alternatively, confinement in porous Vycor glass results in a substantial decrease in the transition temperature ($T_\lambda \simeq 1.95$ K) but no change in critical exponents. Recently studies of the microscopic dynamics of helium confined in aerogel have reported [3,4] a crossover behavior of the roton energy from a low temperature regime ($T < 1.9$ K) with a weak temperature dependence to a high temperature regime, where it exhibits a strong temperature dependence. This anomalous temperature dependence can be understood in terms of a competition between the temperature-dependent roton mean free path and a temperature-independent length scale set by the porous media.

In this Letter we report neutron inelastic scattering measurements of the collective excitation spectrum of superfluid helium confined in porous Vycor glass. We observe a strong excitation similar to the roton observed in the bulk liquid which we shall refer to as the three-dimensional (3D) roton. We also observe additional scattering around the bulk roton minimum but lower in energy. This additional intensity is consistent with a two-dimensional (2D) roton which is confined to the higher density liquid layer near the pore wall [5]. The properties of this 2D roton, which have previously been observed directly (via inelastic neutron scattering) on crystalline substrates such as pyrolytic graphite [6–8], and indirectly (via third sound measurements) on amorphous substrates [9], are consistent with the thermodynamic data (e.g., heat capacity [10–12] and normal fluid fraction [13,14]). However, the scattering we observe on this disordered substrate is lower in energy and has a smaller effective mass.

The measurements were carried out on the IN6 time-of-flight (TOF) spectrometer at the Institut Laue-Langevin in Grenoble, France, and the Fermi Chopper Spectrometer (FCS) at the NIST Center for Neutron Research in Gaithersburg, MD. Using an incident neutron wavelength of 4.12 Å (IN6) and 4.8 Å (FCS) the (elastic) energy resolution is approximately 0.140 meV on each instrument. The TOF data were taken at five temperatures between 500 mK and 1.9 K and converted to $S(Q, E)$ using standard techniques [15]. The instrumental resolution for the spectrometer (IN6) was determined from a low temperature (500 mK) scattering measurement of the bulk liquid where the line shapes are extremely narrow [16]. In bulk helium measurements, where the scattering length is on the order of cm, corrections for multiple scattering must be performed. For helium confined to Vycor (which contains remnant neutron absorbing boron) the absorption length is only of the order of mm. Thus multiple scattering effects are negligible. This strong absorption also prevents us from observing the phonons which occur at lower scattering angles.

The (resolution-broadened) scattering at 500 mK for two scattering angles corresponding to wave vectors near the roton minimum are shown in Fig. 1. The background, consisting of the Vycor plus the aluminum sample can, has been subtracted from the data. There is a large scattering peak at the elastic ($E = 0$) position which indicates that nondiffusive (solid) helium is present, as expected from thermodynamic measurements [10]. Since this scattering involves both helium-helium and
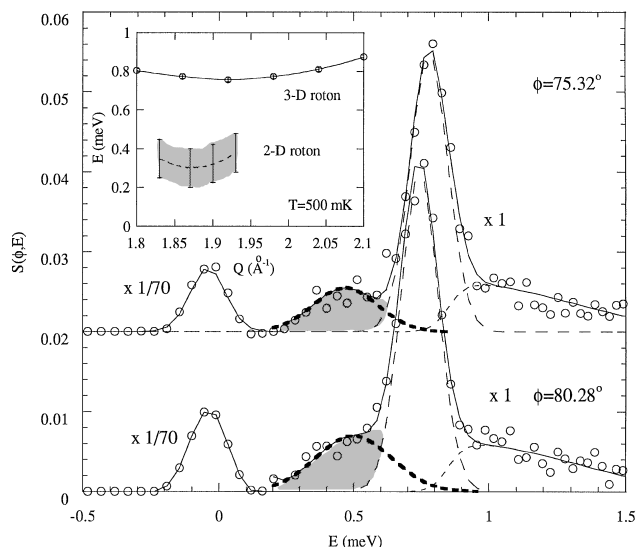
FIG. 1. $S(\phi, E)$ with background subtracted, for two scattering angles, 75.32° and 80.28°, located near the (bulk) roton momentum (1.92 Å^{-1}). Shaded areas indicate additional scattering intensity lower than the bulk roton. Dashed lines denote fits to each individual scattering component (long-dashed line: 3D roton; short-dashed line: multiphonon; bold-dashed line: 2D roton), and the solid line is the sum of these components. Inset: The dispersion of the 3D and 2D rotons (shaded region) extracted from the scattering data.

helium-Vycor correlations and results from the subtraction of two large peaks, we cannot estimate the amount of solid.

A second intense peak, at an energy transfer of about 0.75 meV, is also present whose momentum and energy transfer are consistent with a bulklike, or 3D, roton. The effective mass of the 3D roton, which is determined by the curvature of the dispersion curve (inset in Fig. 1) near the roton minimum, is the same as that in the bulk liquid to within experimental errors. The 3D roton scattering is accompanied by a broad component at higher energies, corresponding to multiphonon processes whose scattering extends from the roton energy upwards. In the bulk, the multiphonon scattering has no significant contribution below the roton energy [16]. Similarly, while multiphonon processes alter the excitation spectrum in helium films, they do not introduce any modes at these low temperatures below the 2D roton energy at similar momentum transfer [17].

An additional contribution to the intensity is observed at energies below the 3D roton in the scattering from the confined liquid. This scattering, which has an energy of 0.3–0.5 meV, has a position, width, and amplitude consistent with theoretical predictions of a localized excitation known as a 2D roton [5,18] which has been proposed to exist within a dense liquid layer adjacent to the solid layer(s) on the pore wall. The density of helium near the pore wall is estimated to be about 0.18 g/cm^3 [13] which corresponds to a roton energy of 0.62 meV in the bulk liq-

uid [19]. Therefore it seems unlikely that the low energy scattering is simply the density shift of the 3D roton energy. A 2D roton has previously been observed directly via neutron inelastic scattering from helium films on crystalline substrates [6,7,20]. Theoretical predictions of the 2D roton energy ($\simeq 0.52$ meV [18]) and experimentally determined values ($\simeq 0.54$ meV [7]) on crystalline substrates are larger than the values we observe in Vycor. The inset of Fig. 1 shows the approximate position of the additional scattering intensity as a function of Q at 0.5 K. The dispersion of this scattering is consistent with a Landau form with a roton energy gap, $\Delta_{2D} = 0.3 \pm 0.2$ meV; wave vector, $Q_R^{2D} = 1.87 \pm 0.10$ Å^{-1}; and effective mass, $\mu = (0.02 \pm 0.13) m_{He}$. Since the intensity is so weak, it is impossible to extract these parameters with much precision. The effective mass cannot be reliably determined due to the large error bars but it seems to be much smaller than values from theoretical predictions [18] or from experimental measurements on crystalline substrates [21]. While there appears to be some difference between the 2D roton parameters found in this experiment and previous measurements on crystalline and amorphous substrates, the uncertainties on these parameters preclude us from making a definitive statement concerning these differences.

The variation with temperature of the 3D roton energy, Δ_{3D}, extracted by fitting a damped-harmonic oscillator line shape [16] (convoluted with the instrumental resolution function) to the scattering at each temperature and momentum transfer, is shown in Fig. 2. The roton energy at low temperature is higher than the bulk liquid value and, although the error bars are large, clearly exhibits a stronger temperature dependence than the bulk liquid. The temperature dependence of the roton energy in the bulk liquid can be described within the theory of Bedell, Pines, and Zawadowski [22] which predicts
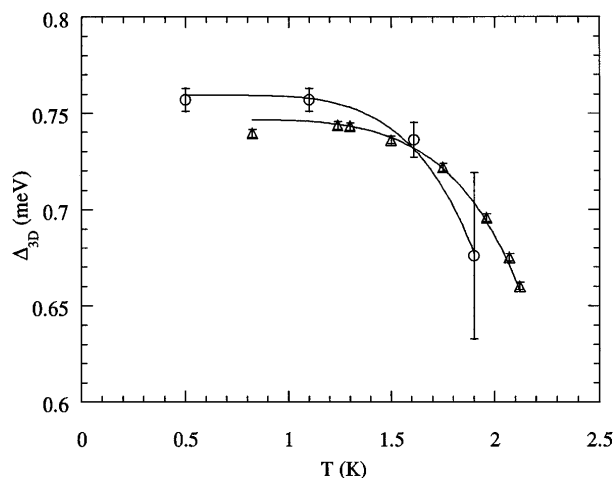
FIG. 2.   Temperature dependence of the (3D) roton energy gap for helium in Vycor (open circles) and bulk helium (triangles) [16,26]. Solid lines are fits to the temperature-dependent roton energy of Bedell et al. [22] as discussed in the text.

$\Delta(T) = \Delta_0 - P_\Delta(1 + R\sqrt{T})\sqrt{T} \exp(-\Delta/T)$, where the bulk values are $\Delta_0 = 0.745$ meV, $P_\Delta = 2.13$, and $R = 0.0603$. Our measurements of the 3D roton in Vycor yield best-fit parameters, shown by the solid line, of $\Delta_0 = 0.759$ meV, $P_\Delta = 1.44$, and $R = 1.479$. The value for R appears in both the expressions for the temperature dependence of $\Delta(T)$ and $\Gamma(T)$ so its value was determined from a simultaneous fit which reduces the correlation among R and the other fit parameters. The P_Δ term is determined by the $\ell = 0$ component of roton-roton scattering, which appears to be suppressed by confinement, while the R term is determined by the cubic corrections to the roton dispersion relation, which appears to be larger here than in the bulk.

The microscopic excitations can be directly related to macroscopic quantities such as the heat capacity and superfluid fraction. For example, for $T > 1$ K the roton is the dominant excitation in determining the heat capacity which, due to the roton energy gap, is proportional to $T^{-3/2} \exp(-\Delta/k_B T)$. Figure 3 shows the heat capacity results plotted so that this behavior yields a straight line with a slope of Δ. Previous thermodynamic measurements have extracted roton energies between 0.48 and 0.53 meV [10,12,14], which are much lower than the bulk value of 0.745 meV, but higher than the energy of the 2D roton (~ 0.3 meV) we have observed.
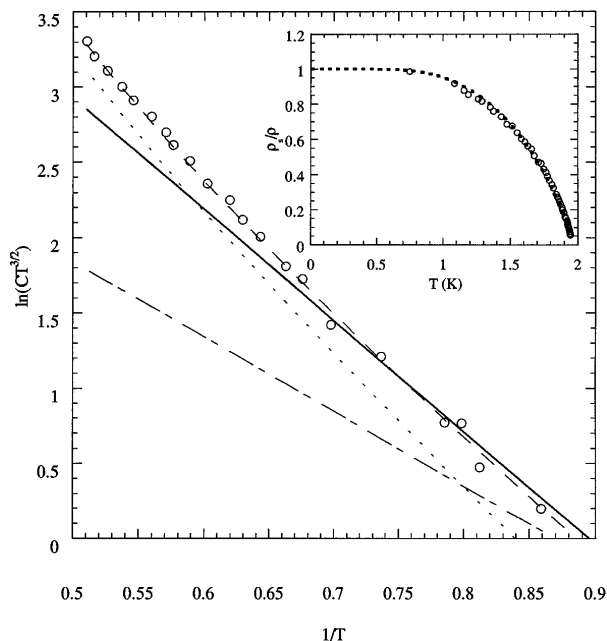
FIG. 3. Heat capacity data (open circles) [11] and superfluid fraction data (inset, open circles) [25] plotted to illuminate the 2D and 3D character in different temperature regimes. The solid line corresponds to $\Delta = 0.52$ meV extracted from the heat capacity measurements. The dashed line is the sum of the 2D (dash-dotted line) contribution and the 3D (dotted line) contribution. The inset shows the superfluid fraction as a function of temperature [25]. The bold-dotted line is a fit of the sum of the 2D and 3D contributions.

It is clear that both the 2D and 3D rotons must be taken into account in determining the macroscopic properties. At low temperature the 2D roton will dominate the behavior due to its lower excitation energy, while at high temperatures the 3D roton will primarily determine the behavior. At intermediate temperatures both the 2D and 3D rotons will contribute to the macroscopic response. The contribution of the 3D roton to the heat capacity is [23]

$$C_R^{3D} = \left(\frac{\mu}{2\pi}\right)^{1/2} \frac{k_B Q_R^2 \Delta_{3D}^2}{\rho \pi \hbar (k_B T)^{3/2}} \exp\left(-\frac{\Delta_{3D}}{k_B T}\right), \quad (1)$$

where μ_{3D}, Δ_{3D}, and Q_R are the effective mass, energy, and momentum of the 3D roton, and ρ is the liquid density (g/cm^3). A similar calculation for the 2D roton gives [24]

$$C_R^{2D} = \left(\frac{\mu_{2D}}{2\pi}\right)^{1/2} \frac{k_B Q_R^{2D} \Delta_{2D}^2}{\sigma \hbar (k_B T)^{3/2}} \exp\left(-\frac{\Delta_{2D}}{k_B T}\right), \quad (2)$$

where σ is the density (g/cm^2) of the higher density liquid layer. A fit of the heat capacity data to a sum of the 2D (using the low temperature value for Δ_{2D}) and 3D [using the measured values for $\Delta_{3D}(T)$] contributions is shown in Fig. 3. The 2D roton has a relative spectral weight of 20% ($\pm 10\%$) compared to the 3D roton in agreement with estimates of the number of atoms in the dense liquid layer at the liquid-solid interface and liquid in the center of the pores. It appears that the estimates of the roton energy previously extracted from heat capacity measurements (~ 0.5 meV) are a weighted average of the 2D (0.3 meV) and 3D (0.745 meV) values. This behavior (20% 2D + 80% 3D) also adequately describes the superfluid fraction data [25] as a function of T as shown in the inset of Fig. 3.

The roton linewidth, shown in Fig. 4, is different from that observed in the bulk. It exhibits both a different temperature dependence than the bulk and a finite value as T goes to zero. In the bulk liquid the roton linewidth is determined by roton-roton scattering [22] and is given by $\Gamma(T) = P_\Gamma(1 + R\sqrt{T})\sqrt{T} \exp(-\Delta/T)$, where $P_\Gamma = 3.59$ meV, which is determined by the full roton-roton scattering. Assuming that the roton linewidth of the confined liquid results from a temperature-independent component, Γ_0, which adds in quadrature to a temperature-dependent component yields an expression for the linewidth of $\Gamma(T) = \{\Gamma_0^2 + [P_\Gamma(1 + R\sqrt{T})\sqrt{T} \exp(-\Delta/T)]^2\}^{1/2}$. A fit of this form, with R constrained to have the same value as for the fit to the 3D roton energy, yields $\Gamma_0 = 0.033$ meV and $P_\Gamma = 3.59$ meV. It is interesting to note that the differences in temperature dependence between the bulk and confined liquid result from changes in R rather than from changes in P_Γ, which is determined by overall roton-roton scattering.

The finite roton linewidth of 0.033 meV at low temperatures reflects an additional temperature-independent
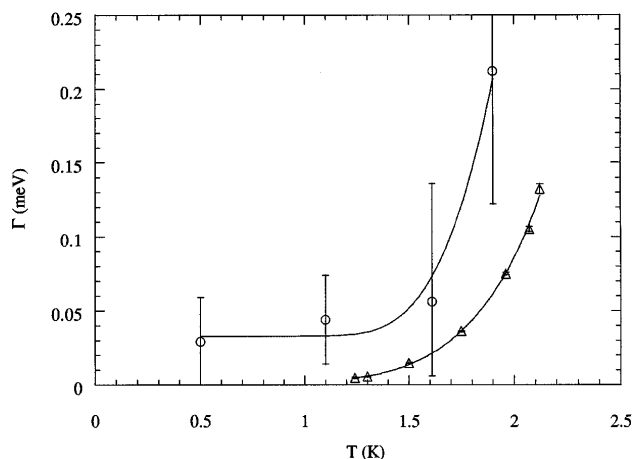
FIG. 4.   Temperature dependence of the roton linewidth for helium in Vycor (open circles) and bulk helium (open triangles) [16,26]. Smooth solid lines are fits to the roton linewidth expression of Bedell *et al.* [22] as discussed in the text.

scattering process. Comparison to the bulk liquid, where roton-roton scattering determines the linewidth, yields a roton mean free path on the order of 500 Å. This mean free path, while of the correct order of magnitude for the confining media, is much larger than the mean pore diameter and a factor of 2 larger than the Vycor pore correlation length. One possible origin of this unexpectedly long mean free path could be elastic scattering of rotons from the surface which might not affect the roton lifetime.

In summary, we have observed additional scattering below the 3D roton which is consistent with a 2D roton, for helium confined in porous Vycor. In addition, we have observed a bulklike 3D roton whose properties are similar to those of the roton in bulk helium but which exhibits a finite linewidth consistent with the confining geometry. We find that when both the 2D and 3D rotons are taken into account we can obtain an adequate description of the macroscopic properties of the confined liquid.

[1] P. J. Bendt, R. D. Cowan, and J. L. Yarnell, Phys. Rev. **113**, 1386 (1959).

[2] M. H. W. Chan, K. I. Blum, S. Q. Murphy, G. K. S. Wong, and J. D. Reppy, Phys. Rev. Lett. **61**, 1950 (1988).

[3] J. DeKinder, G. Coddens, and R. Millet, Z. Phys. B **95**, 511 (1994); G. Coddens, J. DeKinder, and R. Millet, J. Non-Cryst. Solids **188**, 41 (1995).

[4] P. E. Sokol, M. R. Gibbs, W. G. Stirling, R. T. Azuah, and M. A. Adams, Nature (London) **379**, 616 (1996); M. R. Gibbs, P. E. Sokol, W. G. Stirling, R. T. Azuah, and M. A. Adams, J. Low Temp. Phys. **107**, 33 (1997); R. M. Dimeo, P. E. Sokol, C. R. Anderson, W. G. Stirling, and M. A. Adams, Phys. Rev. Lett. **79**, 5274 (1997).

[5] T. C. Padmore, Phys. Rev. Lett. **32**, 826 (1974).

[6] B. Lambert, D. Salin, J. Joffrin, and R. Scherm, J. Phys. (Paris) **38**, L377 (1977).

[7] W. Thomlinson, J. A. Tarvin, and L. Passel, Phys. Rev. Lett. **44**, 266 (1980).

[8] H. J. Lauter, H. Godfrin, and P. Leiderer, J. Low Temp. Phys. **87**, 425 (1992); H. J. Lauter, H. Godfrin, V. L. P. Frank, and P. Leiderer, Phys. Rev. Lett. **68**, 2484 (1992).

[9] J. E. Rutledge, W. L. McMillan, and J. M. Mochel, Phys. Rev. B **18**, 2155 (1978).

[10] D. F. Brewer, A. J. Symonds, and A. L. Thomson, Phys. Rev. Lett. **15**, 182 (1965).

[11] D. F. Brewer, J. Low Temp. Phys. **3**, 205 (1970).

[12] R. H. Tait and J. D. Reppy, Phys. Rev. B **20**, 997 (1979).

[13] D. J. Bishop, J. E. Berthold, J. M. Parpia, and J. D. Reppy, Phys. Rev. B **24**, 5047 (1981).

[14] C. W. Kiewiet, H. E. Hall, and J. D. Reppy, Phys. Rev. Lett. **35**, 1286 (1975).

[15] C. G. Windsor, *Pulsed Neutron Scattering* (Taylor and Francis, London, 1981).

[16] K. H. Andersen and W. G. Stirling, J. Phys. Condens. Matter **6**, 5805 (1994).

[17] B. E. Clements, E. Krotscheck, and C. J. Tymczak, Phys. Rev. B **53**, 12 253 (1996).

[18] W. Gotze and M. Lucke, J. Low Temp. Phys. **25**, 671 (1976).

[19] J. S. Brooks and R. J. Donnelly, J. Phys. Chem. Ref. Data **6**, 51 (1977).

[20] B. E. Clements *et al.*, Phys. Rev. B **53**, 12 242 (1996).

[21] H. J. Lauter, H. Weichert, and C. Tiby, Physica (Amsterdam) **107B**, 239 (1981).

[22] K. Bedell, D. Pines, and A. Zawadowski, Phys. Rev. B **29**, 102 (1984).

[23] J. Wilks, *The Properties of Liquid and Solid Helium* (Clarendon, Oxford, 1967).

[24] W. F. Saam and M. W. Cole, Phys. Rev. B **11**, 1086 (1975).

[25] J. D. Reppy, J. Low Temp. Phys. **87**, 205 (1992).

[26] K. H. Andersen *et al.*, J. Phys. Condens. Matter **6**, 821 (1994).